Constitutive Models for Rubber VI – Heinrich et al. (eds)
© 2010 Taylor & Francis Group, London, ISBN 978-0-415-56327-7

Temperature dependence of Mullins softening-healing phenomena: An outline for theoretical description based on experiments

A.F.M.S. Amin
Civil Engineering Department, Bangladesh University of Engineering and Technology, Dhaka, Bangladesh

A. Lion
Institute of Mechanics, Faculty of Aerospace Engineering, University of Federal Armed Forces Munich, Neubiberg, Germany

ABSTRACT: The influence of the temperature on the Mullins softening effect and its recovery behavior (known as the *healing phenomena*) is experimentally investigated using a rubber blend. To study the influence of low temperatures and large deformations on the Mullins effect, cyclic strain-controlled processes are applied under different temperatures. Experimental results show that low temperature increases both the hysteresis properties and the Mullins effect. The softened specimens are then subjected to a sequence of heating, cooling and conditioning processes in order to study the influence of the temperature on healing phenomena. The results indicate the existence of a threshold temperature: if the specimen temperature is larger than this threshold, a nearly complete recovery of the material occurs within finite time, while any temperature below this limit will be too small for healing. In order to take the temperature dependences of softening-healing effects and their reversibility into account, the paper attempts to outline a thermodynamically consistent theoretical framework to describe these experimentally observed phenomena. In order to preserve the reversible character of the softening effect, fraction of free energy that is dissipated during softening process are described as a function of both temperature and an internal variable. Subsequent derivations lead to the constitutive relations in integral form.

1 INTRODUCTION

1.1 *General*

The Filler-reinforced vulcanized rubber and its blends are frequently-used for engineering applications, e.g. tires, base isolation bearings, air springs, acoustic coatings, tunnel linings for over a century (cf. Morawetz 2000, Amin et al. 2002, 2006). To shape the geometry of these products, geometric nonlinearities need to be considered together with the mechanical properties. The application of a numerical procedure which considers an adequate constitutive model founded on nonlinear continuum mechanics and the principles of thermodynamics (c.f. Haupt 2000) can bring realistic sophistication to a computer aided design and manufacturing process.

The mechanical behavior of filler-reinforced rubber originates from a network of macromolecules containing chemical and physical crosslinks, entanglements and filler particles. The macromolecular network of filler-reinforced rubber exhibits rate-dependent behavior, hysteresis and energy dissipation during monotonic and cyclic deformations. Therefore, the stress response of this material depends strongly on the applied deformation history (Treloar 1973). Lion (1996, 1997a,b) provided experiments and a constitutive model which also consider the temperature. On the other hand, macromolecular networks can change their microstructure at temperatures much higher than cryogenic temperatures (200 K). Such processes are possible in two different ways: 1) the healing of Mullins effect (c.f. Bueche 1961 and Figure 1) and 2) the crystallization process (c.f. Wood and Roth 1944; Wood and Bekkedahl 1946; Gent 1954; Stevenson 1983; Gent and Zhang 2001; Fuller et al. 2004). Both the temperature and the deformation history are the determining factors for the duration needed to complete these changes. The time-, temperature- and deformation-dependent changes in the macromolecular network, however, influence the mechanical material behavior of rubber. Thus, there exists an obvious necessity to extend the experimental knowledgebase of the material over the practical deformation and temperature

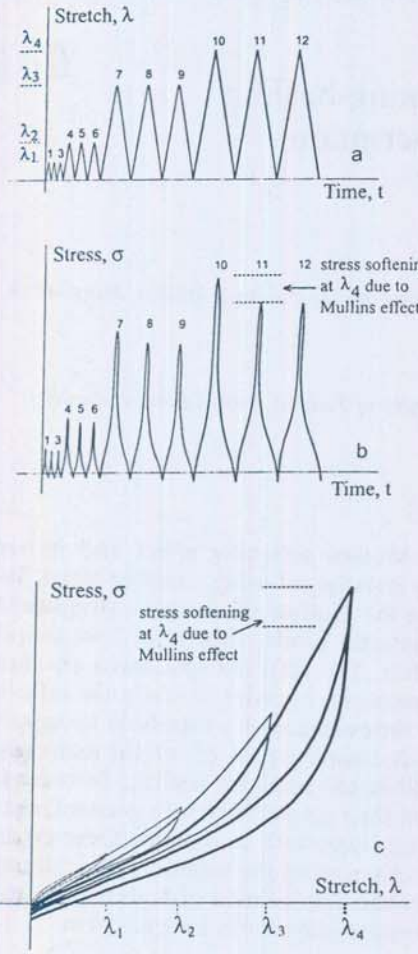

Figure 1. Mullins effect. When a virgin specimen is subjected to a cyclic process with different maximum stretches λ_1, λ_2, λ_3 and λ_4, respectively. The softening, occurring between cycles 10 and 11 in a virgin rubber at the stretch level λ_4, is illustrated in Figs. 1b and 1c. It increases progressively when the material experiences larger stretch amplitudes e.g. $\lambda_1 < \lambda_2 < \lambda_3 < \lambda_4$. At any amplitude lower than the past maximum amplitude, the material exhibits a repeatable stress-strain response with a very little softening in the successive cycles (Lion 1996, Gentot et al. 2004).

ranges such that motivations for founding more general constitutive models can be obtained. This paper examines temperature history dependence of Mullins softening-healing phenomena through experiments and outlines a theory to narrate the experimental facts.

2 EXPERIMENTS

2.1 *Experimental scheme*

We study the thermomechanical behavior of a NR/BR blend. The specimens are tested under

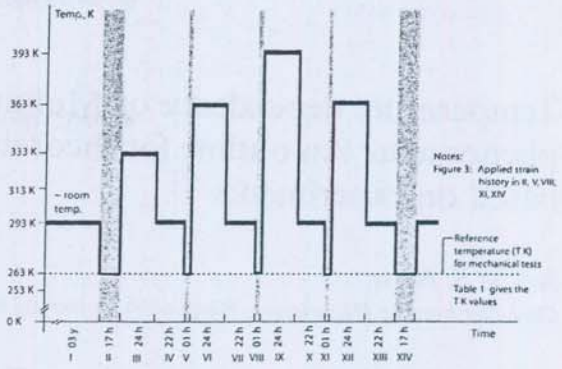

Figure 2. Temperature histories applied to specimens. The figure is to be read in conjunction with Figure 3 and Table 1.

Table 1. Reference temperatures (Figure 2) for mechanical tests.

Sl. no.	Reference temperatures T K
1	253 K
2	263 K
3	293 K
4	313 K
5	333 K

Note: The table is to be read in conjunction with Figs 2 and 3.

tension to understand the effect of the temperature on the mechanical behavior of the blend. In this course, we apply a specified deformation history (Figure 2) on a virgin specimen at a reference temperature and reapply the same deformation history at that reference temperature for a few more times, but also after subjecting the specimens to various temperature histories. By this sequence of events, an insight into the thermorheological processes which occur in the material can be obtained. In this way, the temperature history dependences of the Mullins effect and its healing are investigated under five reference temperatures (Table 1).

2.2 *Temperature dependence of Mullins effect*

Figure 4a shows the effect of the specimen temperature on the first loading cycles (Cycle 1, 3, 5, 7; Fig. 3), while Fig. 4b shows the same effect observed in the second loading cycles (Cycle 2, 4, 6, 8; Fig. 3). The stress amplitudes recorded in the second loading cycles (Fig. 4b) are lesser than those in the first cycles (Fig. 4a). These reductions can be interpreted as the Mullins effect. However, it should be noted that a specimen at a lower temperature may contain a larger crystallinity and a

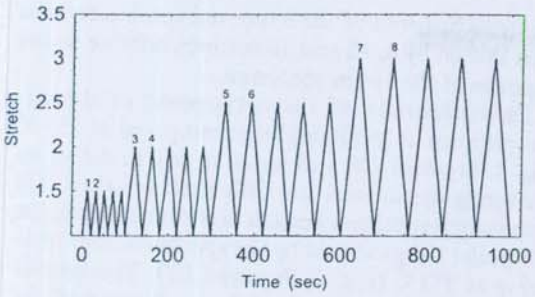

Figure 3. Deformation history applied in specimens at different thermal equilibriums. The figure is to be read in conjunction with Figure 2 and Tables 1. At XIV deformation history was applied only up to 600 s.

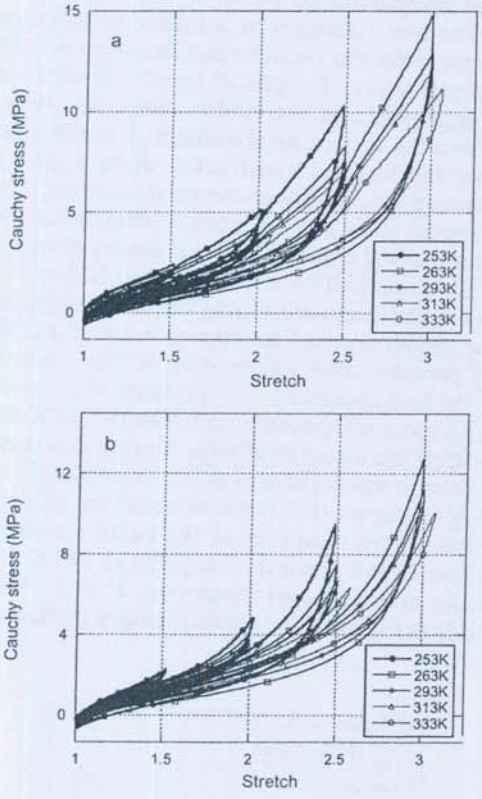

Figure 4. Mullins effect characterized by stretch amplitude dependent softening phenomena at different temperatures. All observations are made 0.05/s stretch rate as per the experimental scheme shown in Figs. 2–3. (a) The first cycles (1, 3, 5, 7); (b) The second cycles (2, 4, 6, 8).

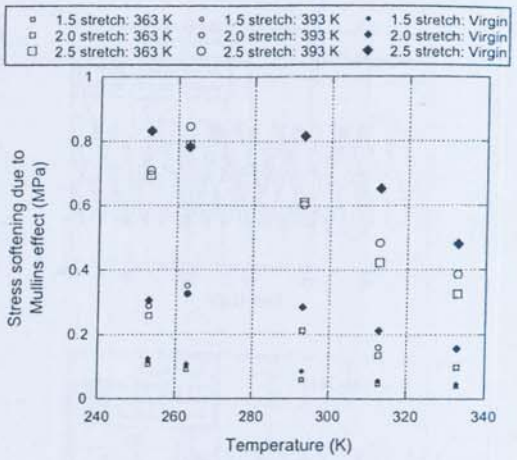

Figure 5. Mullins softening effect is viewed as the difference in stress amplitude over the first and second cycle (stress softening effect). Stress amplitudes at first cycles (1, 3, 5, 7) are deducted from those recorded at second cycles (2, 4, 6, 8) and plotted as a function of temperature. The results from the virgin specimens (at T K) are compared with those after tempering at 363 K and 393 K (Figs. 2–3).

lower amorphicity. In addition, it should have a lower molecular mobility and a larger rate dependence. By taking these points as background, we note that the energy absorption, represented by the areas of the stress-stretch curves of a cycle, is much larger at low temperatures and it decreases with the increase of temperature.

In Figure 5, the maximum stresses recorded in cycles 1, 3, 5, 7 (Figs. 2–3) are compared with those belonging to the cycles 2, 4, 6, 8 (Figs. 2–3) and are plotted as a function of temperature (T K). The plot shows that the softening increases with increasing stretch amplitude and decreasing temperature. A change is observed at temperature levels below 263 K: in comparison with the softening observed at 253 K, the softening is quite small at 333 K. The stress responses of virgin specimens recorded in the tests at 263 K are presented in Figure 6 as functions of time. A diminishing trend of the softening at each stretch amplitude is noted after the second cycles (cycles 2, 4, 6, 8). In addition, the peaks of the stress response clearly depict the deformation dependence of the Mullins effect: the higher the applied stretch the higher is the softening effect. At the end of each cycle, the applied stretch was set to zero (Fig. 2–3). This causes that the stress changes its sign due to viscosity-induced strain rate effects. The stress responses belonging to the other temperatures lead to the same conclusions and are skipped for brevity. These observations (Figure 6) are consistent with the earlier work at room temperature (Lion 1996).

2.3 *Effect of heat treatment temperature on the healing behavior*

The consequences of successive temperature increases during the heat treatment (from 333 K

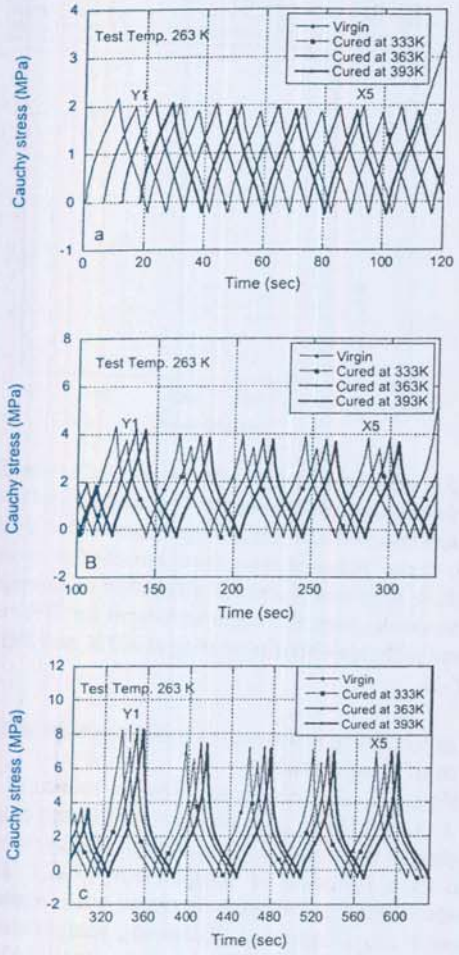

Figure 6. Stress histories obtained from virgin specimen and specimens tempered at different temperatures. The mechanical processes (Figs. 2–3) were applied at 263 K in each of the tests. For the purpose of understandable illustration, the stress histories have been separated from each other by 6 sec. In reporting the stress history for virgin specimen, records only up to first 600 seconds are plotted.

to 393 K; Figure 2, Steps *III, VI, IX*) on the healing behavior of the Mullins effect are also presented in Figure 6. They show different segments of the stress responses corresponding to the different stretch amplitudes. The parameter in these tests is the temperature during the heat treatment which was 24 hours in duration. In performing the mechanical tests, the specimen temperature was held constant at 263 K and the stretch rate was set to 0.05/s. Due to the same stretch rate in all tests, strain-rate effects are not considered. The virgin specimen and tempered specimens were deformed with the stretch history as shown in Fig. 3. During the first 600 seconds both histories are equal. In order to point out the relevant effects in Fig. 6, the stress histories of the tempered specimens have been shifted by 6, 12 and 18 seconds relative to the response of the virgin specimen.

The comparison of the stress peaks of the virgin specimen at 263 K and that tempered at 333 K (Fig. 2, Segment *III*) and tested at 263 K shows an interesting trend: even the fifth peak (marked *X5*) of the virgin specimen lies at a higher value than the first peak (*Y1*) produced by the specimen after tempering at 333 K (Fig. 2, Segment *III*). This amplitude reduction is the result of the application of the further deformation process which the specimen observed before experiencing the heat treatment (Gentot et al. 2004). The effect of the temperature treatment at 333 K is small. But after tempering the specimen at 363 K for 24 hours, the stress peaks become comparable to those of the virgin specimen. The heat treatment at a higher temperature facilitates molecular motions and increases the rate of reconstruction of ruptured bonds between the filler aggregates and the rubber molecules. However, from the current measurements it is not clear whether the bonds reconstructed upon applying temperature are physical or chemical in nature. The experimental data and its interpretation obtained from mechanical tests call for the necessity of measuring the amount of heat which is absorbed or dissipated by the specimens during the heat treatment. Precise measurement of the heat exchange in a DSC device provides more information in this context. After the heat treatment, the specimen was cooled down to room temperature and then to 263 K for performing the mechanical tests. During this cooling process, it was perhaps possible to completely or partially regenerate the crystalline structure. Finally, the stress-stretch responses of the virgin specimen and those of the specimen tempered at 363 K for 24 hours are compared (Segments *II* and *VIII*, Figure 2) in Figure 7: the match is nearly perfect.

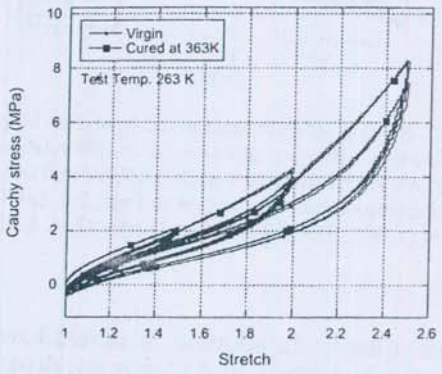

Figure 7. Comparison between the stress-stretch response from virgin specimen and that from the specimen after tempering at 363 K (Figure 2, Segment VI).

A tempering of the specimen at a higher level of 393 K (Figure 2, Segment *IX* and Figure 10) was not found to cause an appreciable increase in the stress amplitude. This observation also demonstrates the existence of a threshold temperature for attaining the virgin material behavior through thermally-activated healing processes. The comparison of the stress responses obtained after tempering the specimen at 333 K, 363 K and 393 K does not suggest any stretch history effect. The significant role of the temperature on the appearance of healing within a specific time interval can thus be recognized.

3 THEORETICAL CONSIDERATIONS

In order to formulate a constitutive theory for the softening-healing phenomena that we observed in experiments, we start with the fundamental laws of thermodynamics in their one-dimensional version. The first law of thermodynamics reads as

$$\rho\dot{e} = \sigma\dot{\varepsilon} - \frac{\partial q}{\partial z} + \rho r \tag{1}$$

The constant ρ is the mass density of the material, e is the specific internal energy density per unit mass, σ is the stress, ε is the strain, $q(z,t)$ is the heat flux in z-direction and r is the heat supply per unit mass. The second law of thermodynamics reads as

$$\rho\theta\gamma = -\rho\dot{\psi} + \sigma\dot{\varepsilon} - \rho s\dot{\theta} - \frac{1}{\theta}q\frac{\partial\theta}{\partial z} \tag{2}$$

where ψ is the free energy density, s is the specific entropy, θ the thermodynamic temperature and γ the internal entropy production which is caused by irreversible processes. The principle of irreversibility states that

$$\gamma \geq 0 \tag{3}$$

for arbitrary thermomechanical changes. To combine both thermodynamical laws, the relation between the internal energy, the free energy and the entropy is needed:

$$e = \psi + s\theta \tag{4}$$

The mechanical part of the free energy function of an unsoftened or virgin nonlinear viscoelastic elastomer can be written as

$$\rho\psi_{mech} = w_{eq}(\varepsilon) + \sum_{k=1}^{n} w_{ovk}(\varepsilon_{ek}). \tag{5}$$

Its equilibrium part $w_{eq}(\varepsilon)$ depends on the total deformation ε and its non-equilibrium part $\sum w_{ovk}(\varepsilon_{ek})$ on the elastic strains of a series of Maxwell elements in parallel. The variables ε_{ek} are the elastic strains of the springs and the ε_{ink} are the inelastic strains belonging to the damping elements:

$$\varepsilon = \varepsilon_{ek} + \varepsilon_{ink} \tag{6}$$

To represent the Mullins effect, we introduce an additional internal variable $0 \leq D \leq 1$ describing the softening behaviour and assume that the loss in the mechanical free energy is not completely dissipated into heat but stored in a different manner in the material:

$$\rho\psi = (1-D)\left(w_{eq}(\varepsilon) + \sum_{k=1}^{n} w_{ovk}(\varepsilon_{ek})\right) + \delta(D,\theta) \tag{7}$$

The function $\delta(D,\theta)$ is that part of the free energy that is released during softening but not dissipated into heat. It has the properties $\delta(0,\theta) = 0$ and $\partial\delta/\partial D \geq 0$. In order to evaluate the second law of thermodynamics, we differentiate the free energy (7) with respect to time

$$\begin{aligned}\rho\dot{\psi} = {} & (1-D)\left\{\frac{\partial w_{eq}}{\partial\varepsilon} + \sum_{k=1}^{n}\frac{\partial w_{ovk}}{\partial\varepsilon_{ek}}\right\}\dot{\varepsilon} - (1-D)\sum_{k=1}^{n}\frac{\partial w_{ovk}}{\partial\varepsilon_{ek}}\dot{\varepsilon}_{ink} \\ & + \frac{\partial\delta}{\partial\theta}\dot{\theta} - \left\{w_{eq}(\varepsilon) + \sum_{k=1}^{n} w_{ovk}(\varepsilon_{ek}) - \frac{\partial\delta}{\partial D}\right\}\dot{D}\end{aligned} \tag{8a}$$

and insert it into (2):

$$\begin{aligned}\rho\theta\gamma = {} & \left(\sigma - (1-D)\left\{\frac{\partial w_{eq}}{\partial\varepsilon} + \sum_{k=1}^{n}\frac{\partial w_{ovk}}{\partial\varepsilon_{ek}}\right\}\right)\dot{\varepsilon} \\ & + (1-D)\sum_{k=1}^{n}\frac{\partial w_{ovk}}{\partial\varepsilon_{ek}}\dot{\varepsilon}_{ink} \\ & - \left(\rho s + \frac{\partial\delta}{\partial\theta}\right)\dot{\theta} - \frac{1}{\theta}q\frac{\partial\theta}{\partial z} \\ & + \left\{w_{eq}(\varepsilon) + \sum_{k=1}^{n} w_{ovk}(\varepsilon_{ek}) - \frac{\partial\delta}{\partial D}\right\}\dot{D}\end{aligned} \tag{8b}$$

In order to satisfy the non-negativity of the specific dissipation $\rho\theta\gamma \geq 0$ for arbitrary thermomechanical processes, i.e. numerical values of the temperature- and strain rates, we obtain the following potential relations for the stress and the entropy:

$$\sigma = (1-D)\left(\frac{\partial w_{eq}}{\partial\varepsilon} + \sum_{k=1}^{n}\frac{\partial w_{ovk}}{\partial\varepsilon_{ek}}\right) \tag{9}$$

$$\rho s = -\frac{\partial\delta}{\partial\theta} \tag{10}$$

The evolution laws for the inelastic deformations and the heat flux are assumed to be

$$\dot{\varepsilon}_{ink} = \frac{(1-D)}{\eta_k} \frac{\partial w_{ovk}}{\partial \varepsilon_{ek}}, \tag{11}$$

$$q = -\lambda \frac{\partial \theta}{\partial z}, \tag{12}$$

which are sufficient conditions for the non-negativity of the corresponding terms in (9). The heat conductivity λ and the viscosities η_k are non-negative constants or functions which have to be determined experimentally. A similar argumentation leads the differential equation

$$\dot{D} = \mu (1-D) \left(w_{eq}(\varepsilon) + \sum_{k=1}^{n} w_{ovk}(\varepsilon_{ek}) - \frac{\partial \delta}{\partial D} \right) \tag{13}$$

modelling the evolution of the internal variable D. The material function μ is non-negative as well and has to be determined on the basis of experimental data. The factor $(1-D)$ has been introduced in (14) in order to constrain $D \leq 1$ The driving force for the evolution of the variable D is the mechanically-stored free energy and the limiting term in (14) is the partial derivative of the function $\delta(D,\theta)$. The simplest constitutive assumption for this derivative is

$$\frac{\partial \delta}{\partial D} = \alpha(\theta) D, \tag{14}$$

where the function $\alpha(\theta)$ describes the temperature dependence of the limiting term. If the mechanical part of the free energy is zero, i.e. $w_{eq}(\varepsilon) + \sum w_{ovk}(\varepsilon_{ek}) = 0$, the material is in mechanical equilibrium. In this case, the rate of the softening variable is negative

$$\dot{D} = -\mu (1-D) \alpha(\theta) D \tag{15}$$

such that the developed constitutive model can represent the temperature-dependent healing of the Mullins effect. Integration of (15) leads to the function

$$\delta = \frac{1}{2} \alpha(\theta) D^2 + h(\theta) \tag{16}$$

and with (11) to the expression

$$\rho s = -\left(\frac{1}{2} \alpha'(\theta) D^2 + h'(\theta) \right) \tag{17}$$

for the entropy. Differentiating (4) with respect to time leads to

$$\rho \dot{e} = \rho \dot{\psi} + \rho s \dot{\theta} + \rho \dot{s} \theta. \tag{18}$$

Considering (8) in combination with (10)–(14) the relation

$$\rho \dot{\psi} = \sigma \dot{\varepsilon} - \sum_{k=1}^{n} \eta_k \dot{\varepsilon}_{ink}^2 - \rho s \dot{\theta} - \frac{\dot{D}^2}{\mu} \tag{19}$$

is obtained for the time rate of the free energy. Inserting this into (19), the expression

$$\rho \dot{e} = \sigma \dot{\varepsilon} - \sum_{k=1}^{n} \eta_k \dot{\varepsilon}_{ink}^2 - \frac{\dot{D}^2}{\mu} + \rho \dot{s} \theta \tag{20}$$

follows for the rate of the internal energy. To derive the equation of heat conduction, we replace $\rho \dot{e}$ in the first law of thermodynamics (1) by (21) and obtain

$$\begin{aligned} -\theta \frac{d}{dt} \left(\frac{1}{2} \alpha'(\theta) D^2 + h'(\theta) \right) &= \lambda \frac{\partial^2 \theta}{\partial z^2} \\ &+ \sum_{k=1}^{n} \eta_k \dot{\varepsilon}_{ink}^2 + \frac{\dot{D}^2}{\mu} + \rho r \end{aligned} \tag{21}$$

which leads to

$$\begin{aligned} -\theta \left(\frac{\alpha''(\theta)}{2} D^2 + h''(\theta) \right) \dot{\theta} &= \lambda \frac{\partial^2 \theta}{\partial z^2} + \sum_{k=1}^{n} \eta_k \dot{\varepsilon}_{ink}^2 \\ &+ \frac{\dot{D}^2}{\mu} + \theta \frac{\alpha'(\theta) D}{2} \dot{D} + \rho r \end{aligned} \tag{22}$$

after rearranging the terms. The factor of the temperature rate on the left-hand side is the specific heat capacity of the material which depends on both the temperature and the internal variable D. The material function $h(\theta)$ can be determined if the specific heat capacity $c_0(\theta)$ of the on the virgin or unsoftened material is known. Integration of

$$-\theta h''(\theta) = c_0(\theta) \tag{23}$$

leads to the expression

$$h(\theta) = h(\theta_0) + (\theta - \theta_0) h'(\theta_0) - \int_{\theta_0}^{\theta} \left(\int_{\theta_0}^{y} \frac{c_0(x)}{x} dx \right) dy \tag{24}$$

for this constitutive function.

4 CONCLUSIONS

Experimental results show that a decrease in the specimen temperature leads to more pronounced hysteresis properties together with an increased softening effect. This observation is rather general in nature and may have a relation to the amount of crystallinity present in the material. Tempering of the softened specimens leads to healing such that the Mullins effect can be observed once again. A comparison of the results obtained from the virgin and the tempered specimens tested at different

temperatures suggests that the Mullins effect shown by the virgin can be healed due heat treatment. However, the tempering of the specimens at elevated temperatures for a specific time showed the existence of a threshold temperature which is necessary to completely heal the specimens.

From our point of view, the experimental data provided in this essay appears to be useful for the future development of physically-based thermo-mechanical material models for filler-reinforced rubber. We have seen that the material behavior of the NR/BR rubber blend does not depend only on the deformation history and the current thermodynamic temperature, but also on the entire temperature history. In addition, healing does occur. To this end, we have presented a thermodynamically consistent phenomenological formulation that has the potential to describe the softening-healing phenomena.

ACKNOWLEDGEMENTS

Dr. A.F.M.S. Amin is grateful to the Alexander von Humboldt foundation for granting a Georg Forster fellowship that enabled him to stay at the Institute of Mechanics, Faculty of Aerospace Engineering, University of the Federal Armed Forces Munich during February 2007–July 2007 to conduct this Joint Collaborative Research. The authors are also much grateful to Mr. P. Höfer for assistance in measurements.

REFERENCES

Amin, A.F.M.S., Alam, M.S., & Okui, Y., 2002. An improved hyperelasticity relation in modelling viscoelasticity response of natural and high damping rubbers in compression: experiments, parameter identification and numerical verification, *Mech. Mater.*, 34, 75–95.

Amin, A.F.M.S., Lion, A., Sekita, S., & Okui, Y., 2006. Nonlinear dependence of viscosity in modeling the rate-dependent response of natural and high damping rubbers in compression and shear: Experimental identification and numerical verification, *Int. J. Plast.*, 22, 1610–1657.

Bueche, F., 1961. Mullins effect and rubber-filler interaction, *J. Appl. Polym. Sci.*, 5, 271–281.

Fuller, K.N.G., Gough, J., & Thomas, A.G. 2004. The effect of low temperature crystallization on the mechanical behavior of rubber, *J. Polymer Science, Part B: Polymer Physics*, 42, 2181–2190.

Gent, A.N., 1954. Crystallization and the relaxation of stress in stretched natural rubber vulcanizates, *Trans. Faraday Soc.*, 50, 521–533.

Gent, A.N., & Zhang, L.Q., 2002. Strain-induced crystallization and strength of rubber, *Rubber Chem. Technology*, 75, 923–933.

Gentot, L., Brieu, M., & Mesmacque, G., 2004. Modeling of stress-softening for elastomeric materials, *Rubber Chem. Technology*, 77, 759–775.

Haupt, P., 2000. Continuum Mechnanics and Theory of Materials, Springer-Verlag, Berlin.

Lion, A., 1996. A constitutive model for carbon black filled rubber: Experimental investigations and mathematical representation, *Continuum Mech. Thermodyn.*, 8, 153–169.

Lion, A., 1997a. A physically based method to represent the thermo-mechanical behavior of elastomers, *Acta Mechanica*, 123, 1–25.

Lion, A., 1997b. On the large deformation behavior of reinforced rubber at different temperatures, *J. Mech. Phys. Solids*, 45, 1805–1834.

Morawetz, H., 2000. History of rubber research, *Rubber Chem. Technology*, 73, 405–426.

Stevenson, A., 1983. The influence of low-temperature crystallization on the tensile elastic modulus of natural rubber, *J. Polymer Science*, 21, 553–572.

Treloar, L.R.G., 1973. The elasticity and related properties of rubbers, *Rep. Prog. Phys.*, 36, 755–826.

Wood, L.A., & Bekkedahl, N., 1946. Crystallization of unvulcanized rubber at different temperatures, *J. Appl. Physics*, 17, 362–375.

Wood, L.A., & Roth, F.L., 1944. Stress-temperature relations in a pure gum vulcanizate of natural rubber, *J. Appl. Physics*, 15, 781–789.